We are IntechOpen, the world's leading publisher of Open Access books Built by scientists, for scientists

4,800
Open access books available

122,000
International authors and editors

135M
Downloads

Our authors are among the

154
Countries delivered to

TOP 1%
most cited scientists

12.2%
Contributors from top 500 universities

CLARIVATE ANALYTICS BOOK CITATION INDEX INDEXED

WEB OF SCIENCE™

Selection of our books indexed in the Book Citation Index in Web of Science™ Core Collection (BKCI)

Interested in publishing with us?
Contact book.department@intechopen.com

Numbers displayed above are based on latest data collected.
For more information visit www.intechopen.com

Chapter 4

Crystallization Kinetics of Bi_2O_3-SiO_2 Binary System

Hongwei Guo

Additional information is available at the end of the chapter

http://dx.doi.org/10.5772/intechopen.74177

Abstract

The Bi_2O_3-SiO_2 glasses were prepared by the melt cooling method. The non-isothermal crystallization kinetics and phase transformation kinetics of the BS glasses were analyzed by the Kissinger and Augis-Bennett equations by means of differential scanning calorimetry (DSC) and X-ray diffraction (XRD). The results show that three main crystal phases, namely $Bi_{12}SiO_{20}$, Bi_2SiO_5, and $Bi_4Si_3O_{12}$ are generated sequentially in the heat treatment process. The corresponding activation energy is 150.6, 474.9, and 340.3 kJ/mol. The average crystallization index is 2.5, 2.1, and 2.2. The crystal phases generated by volume nucleation grow in a one-dimensional pattern, and the metastable Bi_2SiO_5 can be transformed into $Bi_4Si_3O_{12}$, which is in a more stable phase.

Keywords: differential scanning calorimetry, glass-ceramics, non-isothermal, kinetics

1. Crystallization kinetics of Bi_2O_3-SiO_2 binary system

1.1. The structure of bismuth glass and Bi_2O_3-SiO_2 system glass-forming characteristics and structure

Pure Bi_2O_3 cannot form glass, but a small amount of glass formers such as B_2O_3, P_2O_5, and SiO_2 can be used to obtain a melt that condenses into a glassy state [1].

Bismuth ions, similar to lead ions, can enter the network structure of the glass (Bi atom has a similar atomic weight, ionic radius, and electronic configuration as lead atom, both having 2S-electrons on the outer layer). As a glass former, the influence of bismuth on the linear expansion coefficient is not so great if compared to barium and strontium. The glass-forming region of this system is relatively large [1], where the Bi_2O_3/B_2O_3 ratio can reach 2/1 or more. Therefore, when the content of Bi_2O_3 is high enough, it may play a role as a glass former.

The literature [2] studied the formation area of B_2O_3-Tl_2O-Bi_2O_3, B_2O_3-PbO-Bi_2O_3, B_2O_3-CdO-Bi_2O_3 system glass. Glass was melted in a metal crucible, melting amount 2–4 g. This kind of glass is melted in kerosene furnace at 800–900°C for 10–30 min. The resulting glass B_2O_3 content is not high. This proves that the other components act as glass-forming bodies, including Bi_2O_3, PbO, CdO, and Tl_2O. **Figure 1** shows the glass structure of Bi_2O_3-B_2O_3 system at Bi_2O_3 60 mol%. When the concentration of Bi_2O_3 is 75 mol%, the structure is shown in **Figure 2**. It is noteworthy that a more complex structure appears when adding lead oxide to bismuth borate glass, as shown in **Figure 3**. This is because the bismuth ions undergo a severe polarization and deform under the action of an external electric field, thus promoting the formation of asymmetric radicals.

Figure 4 shows the phase diagram of the Bi_2O_3-SiO_2 system [3–5]. By analyzing it, we could found that the Bi_2O_3-SiO_2 system has the properties of forming glass at the molar ratio Bi_2O_3:SiO_2 = 1:1. According to the report by Fei et al. [6, 7], the Bi_2O_3-SiO_2 system glass can be prepared by the conventional glass preparation process at a molar ratio of Bi_2O_3:SiO_2 = 1:1.

Similar to PbO, Bi_2O_3 in the glass structure can significantly reduce the viscosity, increase the density, and can also act as a flux. Bi is a heavy metal element but its field strength is very

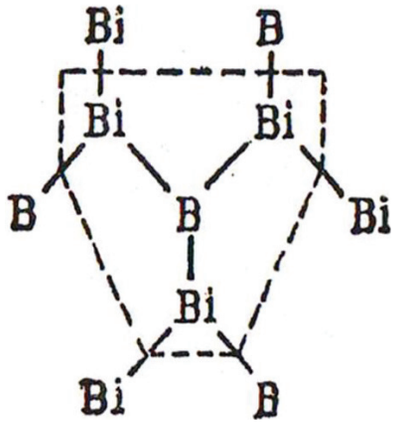

Figure 1. Glass structure of Bi_2O_3-B_2O_3 system at Bi_2O_3 60 mol%.

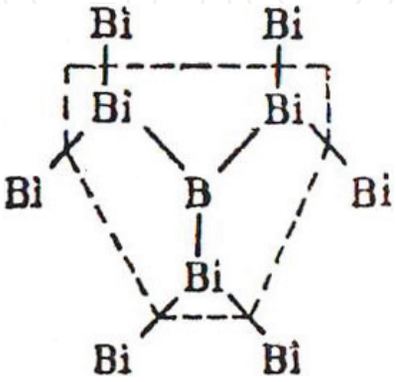

Figure 2. Glass structure of Bi_2O_3-B_2O_3 system at Bi_2O_3 75 mol%.

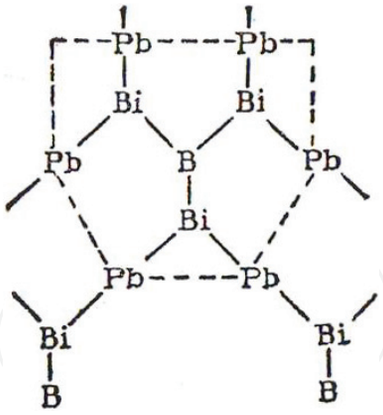

Figure 3. Glass structure of B_2O_3-PbO-Bi_2O_3 system.

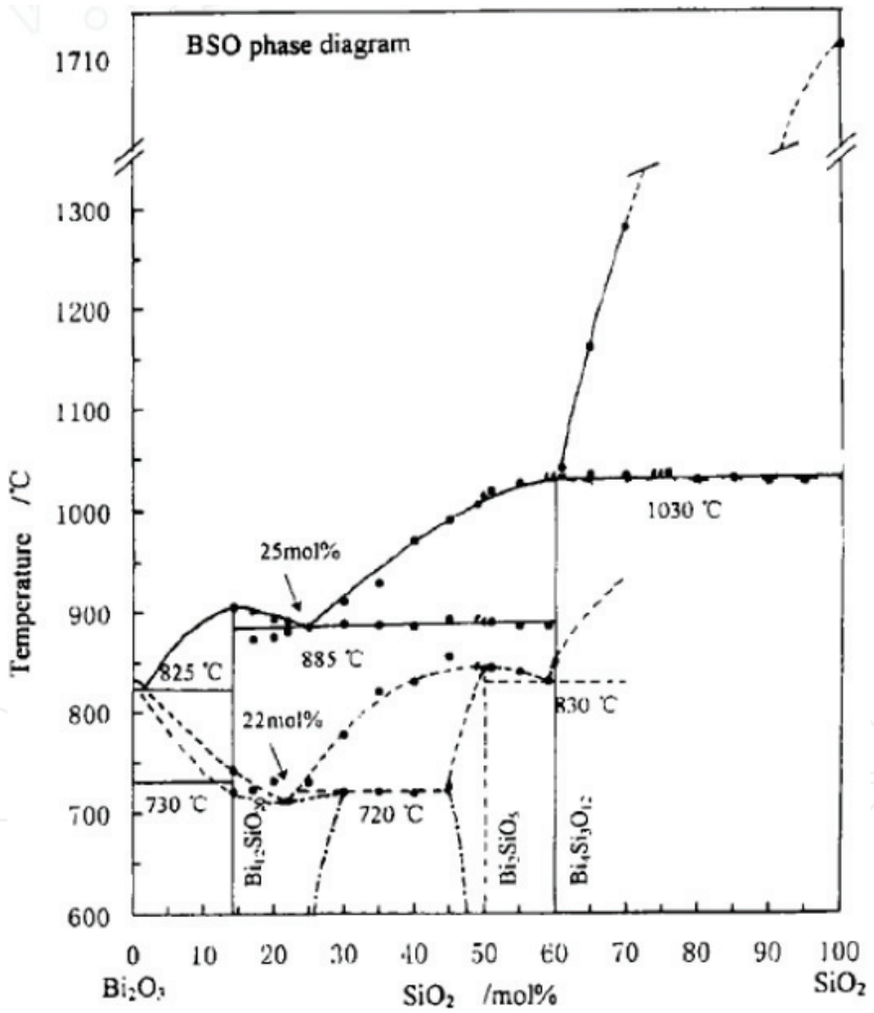

Figure 4. Equilibrium phase diagrams of the Bi_2O_3-SiO_2 system.

small, the bond strength of the Bi-O bond is much stronger than that of the Si-O bond. Therefore, Bi cannot form glass alone but the Bi_2O_3-SiO_2 system glass may have a broad glass-forming region. That is to say the amount of Bi_2O_3 added in this system can be large.

When the mole fraction of Bi_2O_3 is greater than 50%, it is necessary to partially form the glass after water quenching.

Figure 5 shows the XRD patterns of Bi_2O_3-SiO_2 base glasses with a molar ratio of 1:1. The preparation process was as follows: Bi_2O_3 and SiO_2 with a molar ratio of 1:1 were ground for 3 h with absolute ethanol as grinding medium and dried for 1 h. Then, the batch was poured into 200 ml corundum crucible, placed in the box-type electric furnace for melting at 1100°C. Since Bi_2O_3 is volatile, the corundum crucible was capped.

After casting, annealing was carried out at 400°C for 1 h. The annealed glass samples were reddish brown. A part of the samples were ground down to 200 mesh powder.

XRD analysis was carried out. The test conditions were CoK_α radiation, tube voltage 40 kV and current 4 mA, step 0.02°, scanning speed 6°/min, scanning range 10–80°. **Figure 5** shows the typical steamed bun peak. Due to the strong glass forming ability of SiO_2, the Bi_2O_3-SiO_2 system glass is easy to be obtained when the molar ratio of Bi_2O_3/SiO_2 is less than 1.

1.2. Separation of Bi_2O_3-SiO_2 binary system glass

Phase separation, that is, liquid–liquid immiscibility, is a common phenomenon in glass-forming systems [1, 2, 8, 9].

It has been proven that the size of the cationic potential of the network has a decisive effect on phase separation of the oxide glass: when the cation potential Z/r > 1.4 (ion potential refers to the ionic charge number Z and ionic radius r ratio), the system produces liquid–liquid immiscible region above the liquidus temperature. When the value of Z/r is between 1.0 and 1.4, the liquidus is S-type, and there is a metastable immiscible region below the liquidus; when the value of Z/r < 1.0, the phase separation will not happen [2, 8, 9].

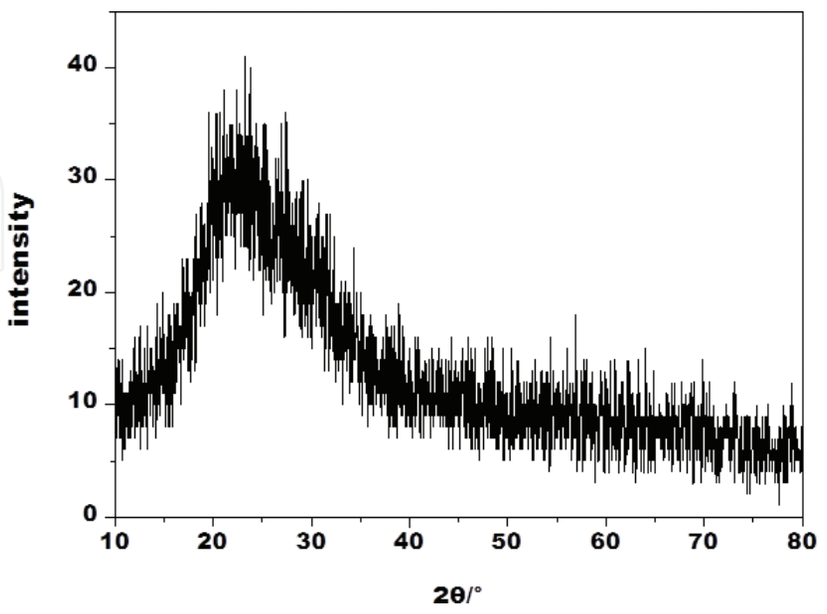

Figure 5. XRD patterns of the Bi_2O_3-SiO_2 system glass.

The cation potential of Bi is Z/r = 3/1.03 > 1.4, which makes it clear that the liquid–liquid immiscible region is generated in the Bi_2O_3-SiO_2 system above the liquidus temperature. Bi is in the seventh main group, and it can expand the phase separation area. Therefore, it is argued that phase separation occurs during the melting of the Bi_2O_3-SiO_2 system glass, resulting in a silicon-rich phase and a bismuth-rich phase. The phase separation in the glass leads to the appearance of new phases, providing favorable nucleation sites and phase separation results in a larger atomic mobility of one of the two liquid phases, which facilitates uniform nucleation. It can be seen that the separation in the Bi_2O_3-SiO_2 system favors the precipitation of crystals in the system.

1.3. Non-isothermal crystallization of Bi_2O_3-SiO_2 (Bi_2O_3:SiO_2 = 1:1) system glass

Figure 6 shows the DSC curves of Bi_2O_3-SiO_2 system glass at different heating rates. There are three distinct crystallization exothermic peaks. At the same time, the temperature of the crystallization peak tends to be stable at heating rate of 10°C/min. In this chapter, a 10 K/min heating rate curve was chosen to determine the heat treatment system of Bi_2O_3-SiO_2 system glass.

From the curves with the heating rate of 10°C/min in **Figure 6**, the three obvious crystallization exothermic peaks were at 564, 659, and 793°C. The heat treatment of the Bi_2O_3-SiO_2 system glass is shown in **Table 1**. Among them, p0 is the basic glass control group, and p1, p2, and p3 correspond to three crystallization peaks from low to high, respectively. Based on the basic glass processing conditions, better crystals can be formed and the type of precipitated crystals can be determined by XRD phase analysis.

The XRD analysis was performed on the samples maintained at different temperatures according to the above heat treatment system. The results are shown in **Figure 7**. Through the

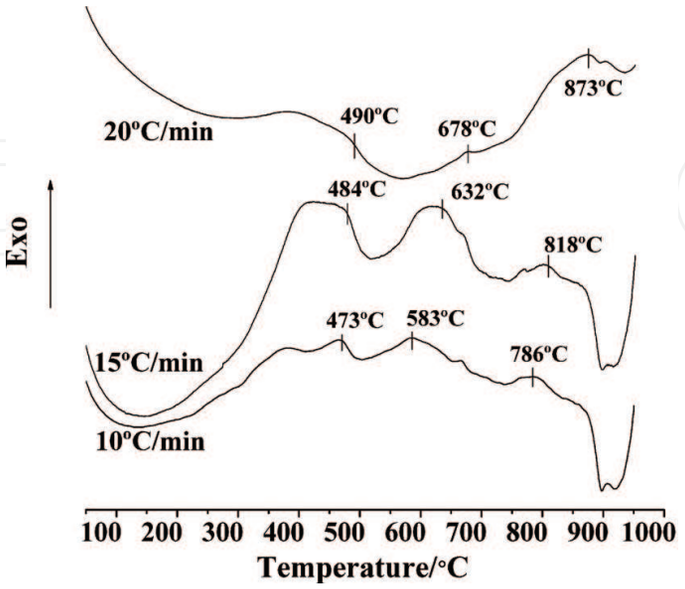

Figure 6. DSC curves of different heating rates of the Bi_2O_3-SiO_2 system (Bi_2O_3:SiO_2 = 1:1).

Heat treatment system	Sample no			
	P0	p1	p2	p3
Nucleation temperature/°C	—	530	630	659
Nucleation time/h	0	1	1	1
Crystal growth temperature/°C	—	564	659	793
Crystal growth time/h	0	3	3	3

Table 1. Heat treatment of the Bi_2O_3-SiO_2 system.

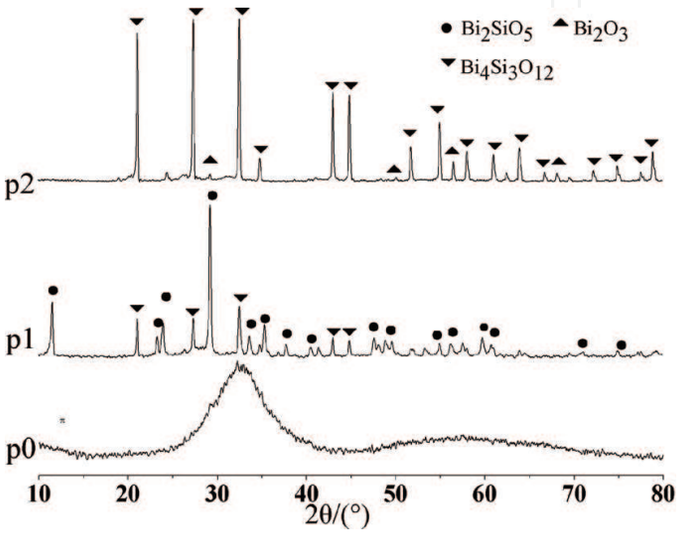

Figure 7. XRD patterns of the samples for different holding time.

comparison with the standard PDF card, it can be seen that the main crystal phase of the p1 sample corresponding to the first crystallization peak on the DSC curve is $Bi_{12}SiO_{20}$, and the minor phase is SiO_2; the main crystal phase of the p2 sample corresponding to the second crystallization peak is Bi_2SiO_5, the secondary crystal phase is $Bi_{12}SiO_{20}$; the main crystal phase of the p3 sample corresponding to the third crystallization peak is $Bi_4Si_3O_{12}$. The results show that the base glass is amorphous, and a diffuse diffraction peak appears in the spectrum. The peak position corresponds to the characteristic peaks of the other three main crystal phases, indicating that there is a short-range ordered structure in the glass, which is considered to be the basis for the separation of the glass [2, 8].

Zhereb et al. divided the liquid state range of the equilibrium diagram of the Bi_2O_3-SiO_2 system into three temperature zones: low-temperature region A, medium-temperature zone B, and high-temperature zone C [3, 5, 10, 11]. Zhereb et al. [5, 12–14] argue that the main crystal phase precipitated in the low-temperature zone A is $Bi_{12}SiO_{20}$, the main crystal phase precipitated in the medium-temperature zone B is Bi_2SiO_5, and the main crystal phase precipitated in the low temperature zone C is $Bi_4Si_3O_{12}$. The abovementioned experimental results are consistent with the conclusions given by Zhereb et al.

1.4. Estimation of thermodynamic properties of Bi_2O_3-SiO_2 melt

At present, no report has been found which focuses on the thermodynamic properties of Bi_2SiO_5 and $Bi_{12}SiO_{20}$. Therefore, it is necessary to estimate the required unknown data for the analysis.

1. c_p**:**

The heat capacity of the solid compound can be approximated as the weighted sum of the solid atomic heat capacity.

$$c = \sum n_i c_i \tag{1}$$

where n_i is the number of i atoms in the compound molecule; and c_i is the atomic heat capacity of the i atom. The atomic heat capacities of Bi, Si and O are shown in **Table 2**.

According to Eq. (1) and **Table 2**, we can calculate that:

$$\begin{aligned} c_p(\ Bi_2SiO_5) &= 2 \times c_p(\mathrm{Bi}) + c_p(\mathrm{Si}) + 5 \times c_p(\mathrm{O}) \\ &= (2 \times 3.6 + 6.4 + 5 \times 4.0)\ \mathrm{cal\ g^{-1}\ K^{-1}} \\ &= 33.6\ \mathrm{cal\ g^{-1}\ K^{-1}} = 140.64\ \mathrm{J\ g^{-1}\ K^{-1}} \end{aligned}$$

$$\begin{aligned} c_p(\ Bi_{12}SiO_{20}) &= 12 \times c_p(\mathrm{Bi}) + c_p(\mathrm{Si}) + 20 \times c_p(\mathrm{O}) \\ &= (12 \times 3.6 + 6.4 + 20 \times 4.0)\ \ \mathrm{cal\ g^{-1}\ K^{-1}} \\ &= 129.6\ \mathrm{cal\ g^{-1}\ K^{-1}} = 542.5\ \mathrm{J\ g^{-1}\ K^{-1}} \end{aligned}$$

From the abovementioned calculation, we know that the c_p of solid Bi_2SiO_5 is 33.6 cal g^{-1} K^{-1} (140.64 J g^{-1} K^{-1}).

Generally, the specific heat of the liquid material is 0.4–0.5 cal g^{-1} K^{-1}, and the material with high specific heat can be taken as large. For example, the specific heat of water can be approximately 1 cal g^{-1} K^{-1}. Therefore, the liquid Bi_2SiO_5 and $Bi_{12}SiO_{20}$ c are taken as 1 cal g K, that is, 4.186 J g^{-1} K^{-1}.

2. ΔH_{fus}

Beijing Institute of Nonferrous Metals Research and Beijing University of Science and Technology Department of Physics and Chemistry jointly proposed to use binary phase diagram calculation system to get the thermodynamic properties [15, 16]. Biostatic equilibrium phase diagram of Bi_2O_3-SiO_2 system can be seen in **Figure 4**. It can be seen that the metastable phase

Atom	Bi	Si	O
c_i	3.6	6.4	4.0

Table 2. Atomic heat capacity (cal·g^{-1}·K^{-1}).

diagram is more complex, including a peritectic reaction and a eutectic reaction. The reaction of precipitating crystals from the liquidus is:

$$A\ (L) + B(L) = C(S) \tag{2}$$

The coefficients of A and B are denoted as p and q. At the beginning of the reaction, the liquid phase composition can be expressed as $\zeta_A + \zeta_B$, at this time $\zeta_C = 0$. At the end of the reaction, $\zeta'_A = \zeta_A\text{-}p\zeta_C$, $\zeta'_B = 0$, $\zeta'_C = \zeta_C$. $x_A = \zeta_A/(\zeta_A + \zeta_B)$, $x_B = \zeta_B/(\zeta_A + \zeta_B)$; $x'_A = (\zeta_A\text{-}p\ \zeta_C)/[\zeta_A\text{-}(p\text{-}1)\ \zeta_C]$. Then, we can get, $x_c = \zeta_B/[q\ \zeta_A\text{-}(p\text{-}1)\ \zeta_B]$, So $x_c/x_B = 1/[q\text{-}(p + q\text{-}1)\ x_B]$.

Then, through further calculations, the following equation can be obtained:

$$\begin{aligned} \frac{dx_c}{dT} &= \frac{(p+q)^2}{q}\ \frac{dx}{dT} \\ \Delta H_{fus} &= \frac{-RT_f^2}{p/(p+q)^2}\ \frac{dT}{dx_B^L} \end{aligned} \tag{3}$$

where R is the gas constant.

The following equation can be obtained by calculated from Eq. (3):

$$\Delta H_{fus}(Bi_2SiO_5) = \frac{1}{4}\left(-8.314 \times 845^2\right) \times \frac{(-1.5)}{526} = 69.716\ \text{kJ g}^{-1}$$

$$\Delta H_{fus}(Bi_{12}SiO_{20}) = \frac{6}{49}\left(-8.314 \times 900^2\right) \times \frac{(-1.402)}{2856} = 26.995\ \text{kJ g}^{-1}$$

So, ΔH_{fus} *(*Bi_2SiO_5*)* = 69.716 kJ g^{-1}, ΔH_{fus} *(*$Bi_{12}SiO_{20}$*)* = 26.995 kJ g^{-1}.

1.5. Crystallization thermodynamics of Bi_2SiO_5 and $Bi_{12}SiO_{20}$ in Bi_2O_3-SiO_2 system

The thermodynamic theory shows that under isothermal pressure:

$$\Delta G = \Delta H - T\Delta S \tag{4}$$

when $\Delta G = 0$, $\Delta H\text{-}T\Delta S = 0$,

$$\Delta S = \Delta H/T_0 \tag{5}$$

where T_0 is the equilibrium temperature of the phase change.

If there is a phase change under unbalanced condition of any temperature T,

$$\Delta H - T\Delta S \neq 0 \tag{6}$$

If ΔH and ΔS do not change with temperature, the following equation can be obtained by taking Eq. (5) into Eq. (6):

$$\Delta G = \Delta H - T\frac{\Delta H}{T_0} = \Delta H\frac{T_0 - T}{T_0} = \Delta H\frac{\Delta T}{T_0}. \tag{7}$$

From Eq. (7), it can be seen that only when $\Delta G < 0$ ($\Delta H \Delta T/T < 0$), the phase change will occur spontaneously. When the phase change is a crystallization exothermic process, $\Delta H < 0$ ($\Delta T > 0$), T_0-$T < 0$. This indicates that the system must be subcooled during the crystallization process.

In this chapter, the enthalpy and entropy change of the crystallization process are calculated at the equilibrium temperature of the system. The enthalpy change and entropy change of the crystallization process are calculated by the irreversible process [17]. Where T is the actual phase transition temperature, T is the equilibrium temperature of the phase change

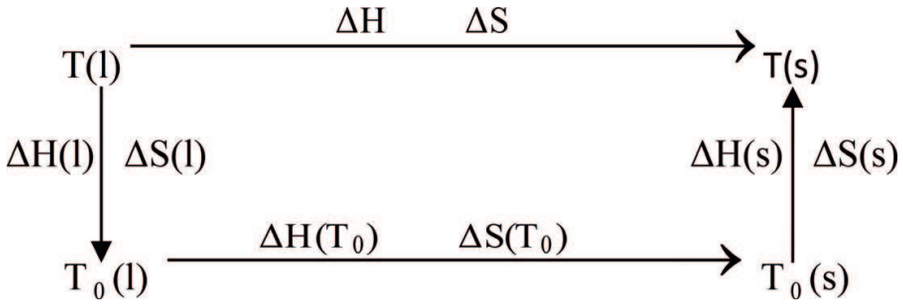

According to this process,

$$\Delta S = \Delta S(l) + \Delta S(s) + \Delta S(T_0) \tag{8}$$

$$\Delta H = \Delta H(l) + \Delta H(s) + \Delta H(T_0) \tag{9}$$

$$\Delta S(l) = \int_T^{T_0} \frac{C_p(l)}{T} dT \tag{10}$$

$$\Delta S(s) = \int_{T_0}^{T} \frac{C_p(S)}{T} dT \tag{11}$$

$$\Delta S(T_0) = \frac{-\Delta_{fus} H(T_0)}{T_0} \tag{12}$$

$$\Delta H(l) = \int_T^{T_0} c_p(l) dT \tag{13}$$

$$\Delta H(s) = \int_{T_0}^{T} c_p(s) dT \tag{14}$$

$$\Delta H(T_0) = -\Delta_{fus} H(T_0) \tag{15}$$

T_0 for Bi_2SiO_5 is obtained from the phase diagram at 845°C, 1118.15 K. Substituting the T_o, c_p, ΔH_{fus} of Bi_2SiO_5 into Eqs. (8)–(15) are calculated as follows:

$$\Delta S(\mathrm{Bi_2SiO_5}) = \Delta S(\mathrm{l}) + \Delta S(\mathrm{s}) + \Delta S(T_0) = \int_T^{T_0} \frac{c_p(l)}{T} dT + \int_{T_0}^{T} \frac{c_p(s)}{T} dT - \frac{\Delta_{fus} H(T_0)}{T_0} \tag{16}$$

$$\Delta S(\mathrm{Bi_2SiO_5}) = (140.64 - 4.186) \times (\ln T - \ln 1118.15) - \frac{69.716 \times 10^3}{1118.15}$$

$$\Delta S(\mathrm{Bi_2SiO_5}) = 136.454 \ln T - 1020.18$$

$$\Delta H(\mathrm{Bi_2SiO_5}) = \Delta H(\mathrm{l}) + \Delta H(\mathrm{s}) + \Delta H(T_0) \tag{17}$$

$$= \int_T^{T_0} c_p(l) dT + \int_{T_0}^{T} c_p(s) dT - \Delta_{fus} H(T_0)$$

$$\Delta H(\mathrm{Bi_2SiO_5}) = (140.64 - 4.186) \times (T - 1118.15) - 69.716 \times 10^3$$

$$\Delta H(\mathrm{Bi_2SiO_5}) = 136.454\ T - 222292.04$$

The above calculated ΔS and ΔH are taken into Eq. (7), ΔT = 145 K, ΔG = −7.478 kJ < 0. This indicates that the process of precipitating Bi_2SiO_5 from the base glass can be carried out spontaneously when the temperature T = T_o-ΔT = 973.15 K.

The same method is used to calculate $Bi_{12}SiO_{20}$, and T for $Bi_{12}SiO_{20}$ was obtained from the phase diagram at 900°C, that is, 1173.15 K:

$$\Delta S(\mathrm{Bi_{12}SiO_{20}Bi_{12}SiO_{20}}) = \Delta S(\mathrm{l}) + \Delta S(\mathrm{s}) + \Delta S(T_0) = \int_T^{T_0} \frac{c_p(l)}{T} dT + \int_{T_0}^{T} \frac{c_p(s)}{T} dT - \frac{\Delta_{fus} H(T_0)}{T_0} \tag{18}$$

$$\Delta S(\mathrm{Bi_{12}SiO_{20}}) = (542.50 - 4.186) \times (\ln T - \ln 1173.15) - \frac{26.995 \times 10^3}{1173.15}\ \Delta S(\mathrm{Bi_{12}SiO_{20}})$$

$$= 538.314 \ln T - 3804.506\ \Delta H(\mathrm{Bi_{12}SiO_{20}}) = \Delta H(\mathrm{l}) + \Delta H(\mathrm{s}) + \Delta H(T_0) \tag{19}$$

$$= \int_T^{T_0} c_p(l) dT + \int_{T_0}^{T} c_p(s) dT - \Delta_{fus} H(T_0)$$

$$\Delta H(\mathrm{Bi_{12}SiO_{20}}) = (538.314 - 4.186) \times (T - 1173.15) - 26.995 \times 10^3$$

$$\Delta H(\mathrm{Bi_{12}SiO_{20}}) = 1538.314\ T - 658518.069$$

The above calculated ΔS and ΔH are taken into Eq. (7), ΔT = 300 K, ΔG = −29.579 kJ < 0. This indicates that the process of precipitating $Bi_{12}SiO_{20}$ from the base glass can be carried out spontaneously when the temperature T = T_o-ΔT = 873.15 K.

It should be noted that, in the abovementioned analysis, c and ΔH values are all estimated. T_0 is obtained from the phase diagram, but the phase diagram of the system has not been fully analyzed, The liquidus in the figure cannot be completely determined, so T_0 and the actual value may also have some error. The calculated value in this chapter can only be used to qualitatively determine how spontaneous the crystallization process is at a certain temperature, not for the precise calculation of crystallization temperature.

1.6. Bi_2O_3-SiO_2 (Bi_2O_3:SiO_2 = 1:1) system glass non-isothermal crystallization kinetics

1.6.1. Crystallization kinetics

Crystallization activation energy E and crystal growth index n are two important parameters to research the crystallization kinetics of glass. The process where glass gradually transforms into the crystal state needs a certain activation energy to overcome the structural rearrangement barrier. The higher is the potential barrier, the greater is the activation energy. Therefore, to a certain extent, the crystallization activation energy reflects the degree of crystallization ability. The crystal growth index n can reflect the nucleation and growth mechanism during the crystallization process.

1.6.2. Crystallization activation energy

In non-isothermal transition, the exothermic peak temperature T_p of the glass on the DSC curve is affected by the heating rate β. When the heating rate is slow, the transition time is sufficient and the process can be carried out at lower temperature, so T_p is lower, and the instantaneous transition rate is small, and the crystallization peak is gentle; when the heating rate is faster, the exothermic peak temperature T_p is correspondingly increased, the instantaneous transition rate is large, and the crystallization peak is sharper [18]. In this chapter, the DSC curves of the samples at the heating rates 5, 10, 15, and 20°C/min were measured. The Kissinger and Ozawa methods were used to calculate the crystallization activation.

(1) Kissinger method to calculate the crystallization activation energy

The kinetics of glass crystallization by DSC method is based on the Johnson-Mehl-Avrami (JMA) equation. Assuming that the reaction mechanism function is $f(x) = (1-x)^n$, the corresponding equation is:

$$\frac{dx}{dt} = K(1-x)^n \tag{20}$$

where n is the reaction order, that is, the crystal growth index, x the phase transition fraction, and K the crystallization rate constant.

The reaction rate constant K follows the Arrhenius relation [19]:

$$K = \mathrm{K}_0^{-\mathrm{E/RT}} \tag{21}$$

where K_0 is the effective frequency factor, E the crystallization activation energy, R the gas constant, and T the absolute temperature.

By the JMA equation, the glass non-isothermal crystallization kinetics can be expressed by the Kissinger Equation [18–20]:

$$\ln\left[\frac{T_p^2}{\beta}\right] = \frac{E}{RT_p} + \ln\left[\frac{E}{R}\right] - \ln K_0 \tag{22}$$

where T_p is the crystallization temperature of the DSC curve and β is the heating rate.

The DSC curves of the Bi_2O_3-SiO_2 system glass at different heating rates are shown in **Table 3**.

According to the Kissinger equation, $\ln(T_p\ \beta)$ and $1/T_p$ is plotted and linearly fitted to obtain the slope E/R. **Figure 8** shows the $\ln(T_p/\beta)$-1/T relationship for the Bi_2O_3-SiO_2 system glass.

From **Figure 8**, the activation energies of the three crystals precipitated in the Bi_2O_3-SiO_2 system glass are: E_{p1} = 150.6 kJ/mol, E_{p2} = 474.9 kJ/mol, and E_{p3} = 340.3 kJ/mol.

(2) Ozawa method to calculate the crystallization activation energy

The Ozawa equation for non-isothermal crystallization of glass can be expressed as:

$$\ln\beta = \frac{-E}{RT_p} + C \tag{23}$$

where E is the crystallization activation energy, T_p the DSC curve crystallization exothermic peak temperature, and C is a constant related to the reaction mechanism function.

A graph of lnβ versus $1/T_p$ is made (**Figure 9**), and a straight line with slope of E/R can be obtained. Then we can calculate the crystal activation energy E.

Heating rate (°C/min)	**5**	**10**	**15**	**20**
Crystalline peak temperature (°C)	547.2	564.0	586.8	593.4
	653.7	659.0	669.3	672.3
	785.2	793.0	812.3	818.1

Table 3. The DSC crystallization peak temperature of Bi_2O_3-SiO_2 system at different heating rates.

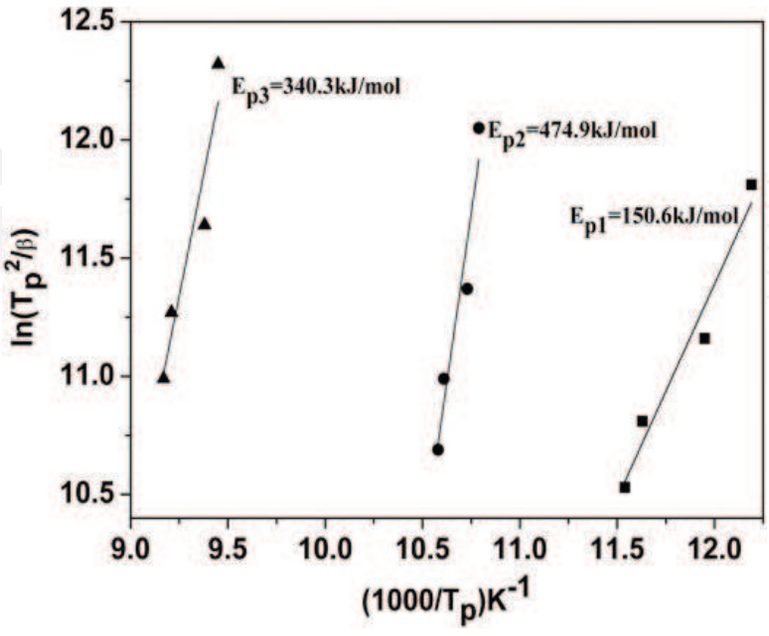

Figure 8. $\ln(T_p^2/\beta)$-$1/T_p$ diagram of Bi_2O_3-SiO_2 glass-ceramics.

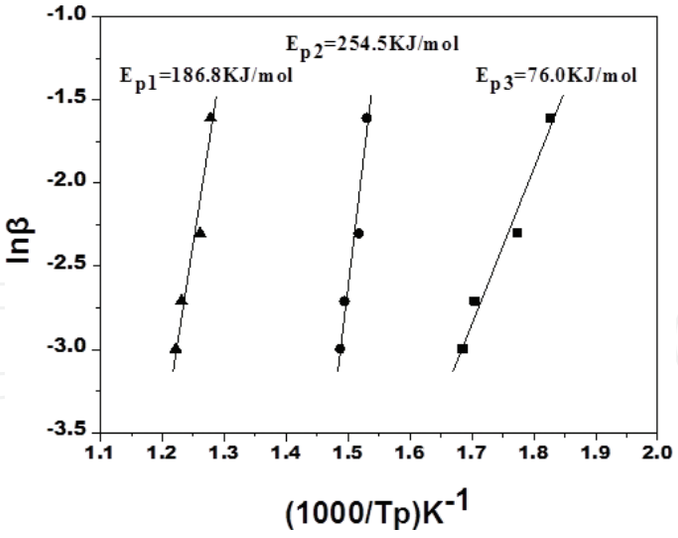

Figure 9. lnβ-1/T_p diagram of Bi_2O_3-SiO_2 glass-ceramics.

From **Figure 9**, the activation energies of the three crystals precipitated in the glass of Bi_2O_3-SiO_2 system are: E_{p1} = 76.0 kJ/mol, E_{p2} = 254.5 kJ/mol, and E_{p3} = 186.8 kJ/mol.

Although the Kissinger method and the Ozawa method generate different activation energy values, the trend is the same. It can be seen that the crystallization ability of $Bi_{12}SiO_{20}$ corresponding to the first crystallization peak (in the low temperature region A) is the strongest, the crystallization ability of the second crystal-forming peak (in the middle-temperature region B) is the weakest, and the crystallization ability of the third crystal-forming peak (in the high-temperature region C) is between the first two peaks.

1.6.3. Crystal growth index

Under the condition that the crystallization activation energy has been determined by the Kissinger method, the crystal growth index n can be obtained by the Augis-Bennett Equation [21, 22]:

$$n = \frac{2.5}{\Delta T} \times \frac{RT_p}{E} \tag{24}$$

where ΔT is the temperature at which the DSC is exothermic at half maximum.

According to the theory of solid phase transition, when n = 4, the way of crystal growth is volumetric nucleation and growth is in three-dimensional space; when n = 3, the way of crystal growth is volumetric nucleation and growth is in two-dimensional space; when n = 2, the way of crystal growth is volumetric nucleation and growth is in one-dimensional direction; when n = 1, the way of crystal growth is surface nucleation, crystals grow in one-dimensional direction on the surface [21, 22].

Table 4 shows the crystal growth indices of the three crystals precipitated in the glass of Bi_2O_3-SiO_2 system at different heating rates. The average growth indices of the three crystals precipitated by the Bi_2O_3-SiO_2 system were $\overline{n}_{p1}$ = 2.5, $\overline{n}_{p2}$ = 2.1, $\overline{n}_{p3}$ = 2.2.

Sample No	Heating rate/(K·min^{-1})				Average crystal growth index
	5	10	15	20	
p1	3.1	2.9	2.1	1.9	2.5
p2	3.0	2.2	1.6	1.5	2.1
p3	2.4	2.1	2.2	2.2	2.2

Table 4. Crystallization index of BS glass-ceramics under different heating rates.

The crystal growth index n can be expressed as

$$n = a + bc \tag{25}$$

where a corresponds to the nucleation rate, and when $a = 0$, the nucleation rate is zero; when $a > 1$, the nucleation rate increases; when $a < 0$, the nucleation rate decreases. b reflects the crystallization mechanism, $b = 0.5$, indicating that the crystallization by the diffusion mechanism control; $b = 1$, the crystallization by the interface control. C represents the grain growth dimension and c = 1, 2, and 3 represent one-dimensional, two-dimensional and three-dimensional growth, respectively.

As we can see, C = 1, b = 0.5, a > 1; therefore, the value of a is the smallest when the crystallization temperature is in the middle temperature region B, and the value of n is shown in **Table 4**. When the crystallization temperature is in the low-temperature zone A, the value of a is the largest. This is consistent with the crystallization ability of the three crystal phases. In the process of melting of Bi_2O_3-SiO_2 system glass, the phase separation occurs, which leads to the emergence of new phase boundary, which in turn provides favorable nucleation sites for nucleation. Therefore, the crystallization process is mainly controlled by diffusion.

The abovementioned analysis shows that the way of Bi_2O_3-SiO_2 glass system crystallization is volumetric nucleation and growth is in one-dimensional space. The crystallization process is mainly affected by diffusion, and the nucleation rate is the highest when the crystallization temperature is in the low-temperature zone A and the lowest when the crystallization temperature is in the medium-temperature zone B.

2. Summary

1. Bi_2O_3-SiO_2 system glass and metastable crystal Bi_2SiO_5 were prepared by high-temperature melt cooling method. During the heat treatment, three main crystal phases were produced in this order: $Bi_{12}SiO_{20}$, Bi_2SiO_5, and $Bi_4Si_3O_{12}$. There are three distinct crystallization exotherms in the DSC curve.

2. The crystallization kinetics of $Bi_{12}SiO_{20}$ and Bi_2SiO_5 were calculated and analyzed. The results show that the crystallization process can be carried out spontaneously at 873 and 973 K, respectively.

3. The Kissinger equation was used to calculate the crystallization activation energy of the base glass and the results are E_{p1} = 150.6 kJ/mol, E_{p2} = 474.9 kJ/mol, and E_{p3} = 340.3 kJ/mol. The Ozawa equation was used to calculate the crystallization activation energy of the base glass and the results are E_{p1} = 76.0 kJ/mol, E_{p2} = 254.5 kJ/mol, and E_{p3} = 186.8 kJ/mol. The calculation results of the two methods show that the crystal phase $Bi_{12}SiO_{20}$ in the low-temperature zone A has the strongest crystallization ability and the crystal phase Bi_2SiO_5 in the medium-temperature zone B has the weakest crystallization ability. The average crystallization index of three kinds of crystals was calculated by Augis-Bennett equation and the results are $\overline{n}_{p1}$ = 2.5, $\overline{n}_{p2}$ = 2.1, and $\overline{n}_{p3}$ = 2.2, respectively. The crystallization process is mainly affected by diffusion.

Author details

Hongwei Guo[1,2]*

*Address all correspondence to: 03guohongwei@163.com; guohongwei@sust.edu.cn

1 Glass Physics and Chemistry, China Electronic Glass Association, China

2 Shaanxi University of Science and Technology, Material Science and Engineering Academy, Xian, China

References

[1] Chen SS. Fusible Glass. China Building Industry Press; 1975:31-60

[2] Nie CS. Practical Glass Components. Tianjin Science and Technology Press; 2001:424-428

[3] Zhereb VP, Skorivo VM. Metastable states in bismuth-containing oxide systems [J]. Inorganic Materials. 2003;**39**(2):121-145

[4] Pastukhov EA, Istomin SA, Belousova NV, et al. Physicochemical properties of Bi_2O_3-Fe_2O_3 and Bi_2O_3-V_2O_5 melts. Rasplavy. 2000;**1**:8-13

[5] Zhereb VP, Skorivo VM. Metastable states in bismuth-containing oxides systems. Inorganic Materials. 2003;**39**(2):25-121

[6] Fei YD, Fan SJ. Research progress of phase relationship and behaviors of Bi_2O_3-SiO_2 system. Journal of Inorganic Materials. 1997;**l2**(4):469-476

[7] Fei YD, Fan SJ, Sun RY. Phase diagram of Bi_2O_3-SiO_2 system. Journal of Inorganic Materials. 1998;**13**(6):798-802

[8] Hu ZQ. Inorganic Materials Science Basic Tutorial. Chemical Industry Press. 2004;**232**:84-86

[9] Zhao YZ, Yin HR. Glass Technology. Chemical Industry Press. 2006;**64**(61):9-10

[10] 刘超, 张昌龙, 周卫宁, Liu C, Zhang CL, Zhou WN. Hydrothermal method to generate colorless BSO crystals. Journal of Synthetic Crystals. 2009;**38**(2):291-295

[11] Cai MQ, Yin Z, Zhang MS, et al. First-principles study of ferroelectric and nonlinear optical property in bismuth titanate. Chemical Physics Letters. 2005;**401**(4-6):405-409

[12] Zhereb VP, F Kargin Y, Skorikov VM. Structural model of Bi_2O_3-AO_2 (a= Si, Ge) melts, Izv. Akad. Nauk SSSR, Neorganicheskie Materialy. 1978;**14**(11):2029-2031

[13] Zhereb VP. Physicochemical study of metastable range phase equilibrium in the systems Bi_2O_3-AO_2 (A=Si, Ge, Ti). Cand. Sci. (Chem.) Dissertation, Moscow: Kurnakov Institute of General and Inorganic Chemistry, Russian Academy of Sciences; 1980

[14] Zhereb VP, Skorivo VM. Effect of metastable phases on the structural perfection of single crystals of stable bismuth oxide compounds. Inorganic Materials. 2003;**39**(11):1365-1372

[15] QB Wang, GY Guo. Liquid and solid matter heat capacity estimation and simple determination method [J]. Contemporary chemical industry. 1985;(4):21-24

[16] Sun GR, Li WC. Prediction of rare earth oxide heat of fusion by binary phase diagram. Chinese Journal of Rare Earths. 1991;**9**(2):117-121

[17] Wang ZL, Zhou YP. Physical Chemistry. Higher Education Press; 2001. 120-122

[18] Lu JS, Dong W. Crystallization dynamics and heat treatment process of LiAlSi based transparent glass [J]. Journal of Nanchang Hangkong University. 2009;**23**(3):5-12

[19] Kissinger HE. Reaction kinetics in differential thermal analysis [J]. Analytical Chemistry. 1957;**29**(11):1702-1706

[20] Lu JS, Dong W. Crystallization behavior and properties of ternary nucleating agent Li_2O-Al_2O_3-SiO_2 system glass. Functional Materials. 2006;**37**(2):156-159

[21] Augis JA, Bennett JE. Calculation of the avrami parameters for heterogeneous solid state reaction using a modification of the Kissinger method. The Journal of Analysis. 1978;**13**: 283-292

[22] Yin HR, Lv CZ, Li H. Phase transformation kinetics of LAS transparent glass—Ceramic with zero phosphorus expansion [J]. Functional Materials. 2009;**40**(1):92-96